

Effects of carbon nanotubes and its functionalization on the thermal and flammability properties of polypropylene/wood flour composites

Shenyuan Fu · Pingan Song · Haitang Yang ·
Yongming Jin · Fengzhu Lu · Jiewang Ye ·
Qiang Wu

Received: 14 December 2009 / Accepted: 6 March 2010 / Published online: 20 March 2010
© Springer Science+Business Media, LLC 2010

Abstract In this article, pristine carbon nanotubes (CNTs) and hydroxylated CNTs (CNT-OH) were employed to enhance the thermal stability and flame retardancy of polypropylene (PP)/wood flour composites (WPC) compatibilized by maleic anhydride-grafted polypropylene (PP-g-MA). Incorporating 10 wt% PP-g-MA only enhanced the mechanical and thermal properties to some extent, but did not improve the flame retardancy of WPC. Thermogravimetric analysis (TGA) showed that the thermal stability of WPC was further increased with the addition of CNTs or CNT-OH and the increase of their loading level. Cone calorimeter measurements suggested that CNTs and CNT-OH could effectively reduce the peak heat release rate (PHRR) of WPC, and the flame retardancy properties reached the optimum value when both of their loading was 1.0 wt%, for instance, a reduction in PHRR by 16.7% and 25% for CNTs and CNT-OH, respectively. In addition, CNT-OH conferred better flame retardancy on WPC relative to pristine CNTs due to the better interfacial adhesion with wood flour and PP matrix, which was evidenced by scanning electron microscopy (SEM) observations.

Introduction

In the past few decades, wood flour or fibers-plastics composites (WPC) have attracted much attention because of their relatively lower cost, density, and lower moisture absorption, as well as better dimensional stability relative to both wood and plastics [1, 2]. On the other hand, environmental concerns caused by waste wood and plastics are another driving force for the development of WPC [3]. Recently, the WPC market experiences a rather rapid development, especially in construction and automobile industries [4].

In the development process of WPC, the interfacial incompatibility between wood and plastics initially causes the poor mechanical properties of WPC [5]. Thus, many efforts have been devoted to the improvement in interfacial adhesion through employment of coupling agents including silanes, titanate, maleic anhydride, and the corresponding grafting polymers [6–9]. However, it is not enough for WPC to possess only good mechanical performance, since wood components and plastic like polypropylene and polyethylene are inherently inflammable, which will inhibit their wide applications in construction especially in housing and automobile fields.

In the case of WPC, few efforts have been made to reduce its flammability, and thus, we still have a long way to go. Because of the environmental concerns arising from halogenated flame retardants (FRs), processing problems, and poor mechanical performances from traditional flame retardants like aluminum trihydrate (ATH) and magnesium hydroxide (MH) due to their relative loading, the production processes of flame retardants are gradually shifting away from those of traditional FRs [10]. Intumescence flame retardants like ammonium polyphosphate (APP) and its derivatives are reported by many researchers to impart

S. Fu · P. Song (✉) · Y. Jin · F. Lu · J. Ye · Q. Wu
National Engineering & Technology Research Center
of Wood-Based Resources Comprehensive Utilization,
College of Engineering, Zhejiang Forestry University,
Hangzhou 311300, China
e-mail: pingansong@gmail.com

H. Yang
College of Material, Chemistry and Chemical Engineering,
Hangzhou Normal University, Hangzhou 310036, China

good flame retardancy to WPC [11, 12]. However, incorporating APP (30–40 phr) also reduced the Izod impact strength of the composites despite not affecting their tensile strengths [13].

Nanocomposites based on layered silicated nanoparticles like clay and carbon nanotubes have been reported to confer good flame retardancy on polymeric materials at very low loading level [14–19]. For clay-based polymer nanocomposites, the addition of clay could simultaneously improve the flame retardancy and mechanical performance. In the case of WPC, Guo et al. [4] found that incorporating nanoclay particles could enhance the char formation of WF/mPE composites when burned. Their another study showed that a small amount of nanoclay (<0.5 wt%) could remarkably enhance the flame retarding performance and that exfoliated nanocomposites exhibited better flame retardancy than did intercalated and conventional nanocomposites with the same clay content [20]. Zhao et al. [2] reported that the addition of nanoclay could improve strongly the flame retardancy and smoke suppression of PVC/wood flour composites. Since carbon nanotubes (CNTs) could considerably enhance the thermal stability and reduce the heat release rate of PP at very low loading (usually below 1.0 vol%), which was primarily reported by Kashiwagi et al. [18, 19] could CNTs improve the flame retardancy of PP/wood flour composites?

Unfortunately, relatively few efforts have been devoted to investigating the flame retardancy effect of CNTs on WPC to date. Thus, this study mainly focused on investigating the effects of CNTs on the thermal and flame retardancy of PP/wood composites. In addition, in order to improve the dispersion of CNTs in polymeric matrix, the CNTs were functionalized to create hydroxylated CNTs (CNT-OH) and then studied to investigate its flame

retardancy effects with respect to pristine CNTs. Finally, the corresponding flame retardancy mechanism was also discussed.

Experimental

Materials

Polypropylene (PP) (M_w : 280,000, M_n : 58,000) was purchased from Shanghai Petrochemicals Factory. The compatibilizer, PP-grafted maleic anhydride (PP-g-MA), (M_n : 21000, MA: 1.0 wt%) was obtained from Shanghai Rizhisheng Co Ltd. Wood flour was sawdust of poplar with a size of 60–100 mesh, which came from the Hangzhou Wood Processing Plant. Carbon nanotubes (CNTs, 20–30 nm in diameter and 5–10 μm in length) were bought from Chengdu Organic Chemistry Co Ltd. The hydroxylated CNTs (CNT-OH) were self-made according to the methods previously reported [21].

Fabrication of PP/wood flour/CNTs composites

Prior to use, wood flour was dried under reduced pressure at 80 °C for 12 h. A series of nanocomposites were prepared via melt blending PP with a certain amount of wood flour, PP-g-MA, and CNTs or CNT-OH at 180 °C in ThermoHaake mixer with a screw speed of 60 rpm, and the mixing time for each sample was 10 min. The mixed samples were transferred to a mold and preheated at 180 °C for 5 min, then pressed at 15 MPa followed by cooling them to room temperature while maintaining the pressure for 5 min. The obtained sample sheets were used for further measurements. The sample identification and formulations are listed in Table 1.

Table 1 Formulations for PP/wood/carbon nanotubes (CNTs) composites

Identification	PP (wt%)	Wood flour (wt%)	PP-g-MA (wt%)	CNTs (wt%)	TS (MPa)	EB (%)
PWF	60	40	0	0	17.5	14
PWP	50	40	10	0	33.7	23
PWPC-0.5	49.5	40	10	0.5 ^a	37.9	17
PWPC-1.0	49	40	10	1.0 ^a	35.5	13
PWPC-2.0	48	40	10	2.0 ^a	31.3	11
PWPCO-0.5	49.5	40	10	0.5 ^b	40.4	20
PWPCO-1.0	49	40	10	1.0 ^b	39.8	18
PWPCO-2.0	48	40	10	2.0 ^b	38.8	15

Note: All data reported here were the average values

TS tensile strength, EB elongation at break

^a Pristine CNTs

^b CNT-OH

Characterization

Scanning electron microscope (FEI Sirion FESEM) and transmission electron microscope (TEM, JEM-1200EX) were employed to observe the dispersion of wood flour and CNTs or CNT-OH in PP matrix, and the microstructure of the residual chars collected after cone calorimeter tests. Thermogravimetric analysis (TGA) was performed on a TA STD Q600 thermal analyzer at a heating rate of 20°C/min with a scan range from 50 to 600°C in air atmosphere, and each specimen was done in triplicate. Cone calorimeter tests were performed using FTT, UK device according to ISO 5660 at a heat flux rate of 35 kW/m², and the size of specimens was 100 × 100 × 3.0 mm, each sample being performed in triplicate. The data reported herein were the averages of the triplicate experiments. Infrared spectrum (IR) was recorded on a Vector-22 FTIR spectrometer using KBr pellet technology.

Results and discussion

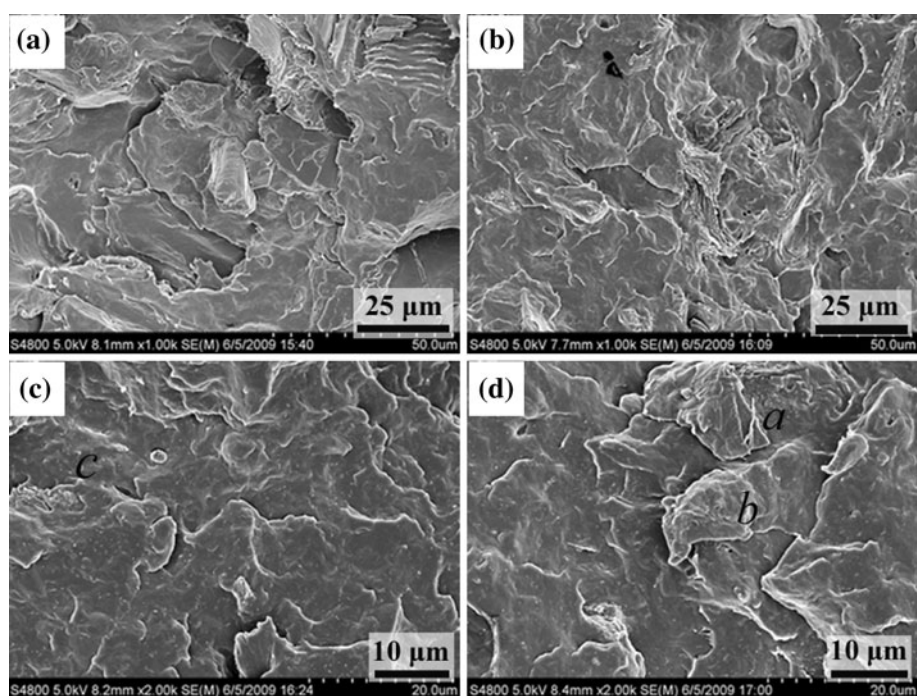
Dispersion of wood flour and CNTs or CNT-OH in the matrix

As shown in Fig. 1, for noncompatibilized system PWF (Fig. 1a), separate wood chips and polymer phase could be clearly observed, indicating poor interfacial compatibility between wood and PP matrix. In contrast, it was obvious that incorporation of PP-g-MA rendered the phase

interfaces indistinct, which demonstrated that the compatibilizer remarkably improved the interface interactions and the dispersion of wood flour in PP matrix (see PWP in Fig. 1b). The case was due to the compatibilization reaction of maleic anhydride groups in PP-g-MA macromolecules with hydroxyl groups on the surface of wood, which has been verified by many researchers [3, 5, 22]. In general, the dispersion of fillers and their interfacial adhesion with the matrix strongly affect the mechanical and other performance of a composite. As seen in Table 1, compared with PWF without the compatibilizer, PWP with 10 wt% PP-g-MA exhibited significant improvement in mechanical properties, for instance, tensile strength and elongation at break were enhanced by 93% (33.7 MPa) and 64% (23%), respectively.

As shown in Fig. 1c and d, both CNTs and CNT-OH could disperse well in the matrix, and the biggest difference between them was in the place where they resided. CNTs primarily located in the PP phase (marked by c in Fig. 1c) due to their close polarity, while CNT-OH could reside in the PP matrix and the interfaces between wood and PP (marked by a & b in Fig. 1d). The latter case was due to the fact that, on one hand, the –OH groups on the surface of CNT-OH had good compatibility with strong polar wood, and on the other hand, CNT-OH could also react with the compatibilizer PP-g-MA which may render CNTs disperse well in PP matrix. As for mechanical performance, the addition of both CNTs and CNT-OH could increase the tensile strengths and elongation at break of WPC. The reinforcement effect of the latter was more

Fig. 1 Dispersion of wood flour and CNTs or CNT-OH in PP matrix



obvious than that of the former, which in turn proved that better interfacial adhesion results in better mechanical properties. With regard to their effects on the thermal and flame retardancy properties, they will be in detail discussed in the next section.

Effects of CNTs or CNT-OH on thermal stability of WPC

Since WPC are usually used in atmospheric air, it is more significant to study their thermal stability in air than in nitrogen atmosphere, Fig. 2 shows the TGA and DTG curves of different WPC in air condition. As is seen in Fig. 2a and b, the noncompatibilized WPC start to degrade at about 272 °C and the maximum weight loss temperature (T_{\max}) occurs at 360 °C. Though the addition of PP-g-MA slightly decreased the initial degradation temperature of WPC (ca. 269 °C), it remarkably extended the T_{\max} up to 384 °C, which indicated that compatibilization could contribute to the thermal stability to certain extent.

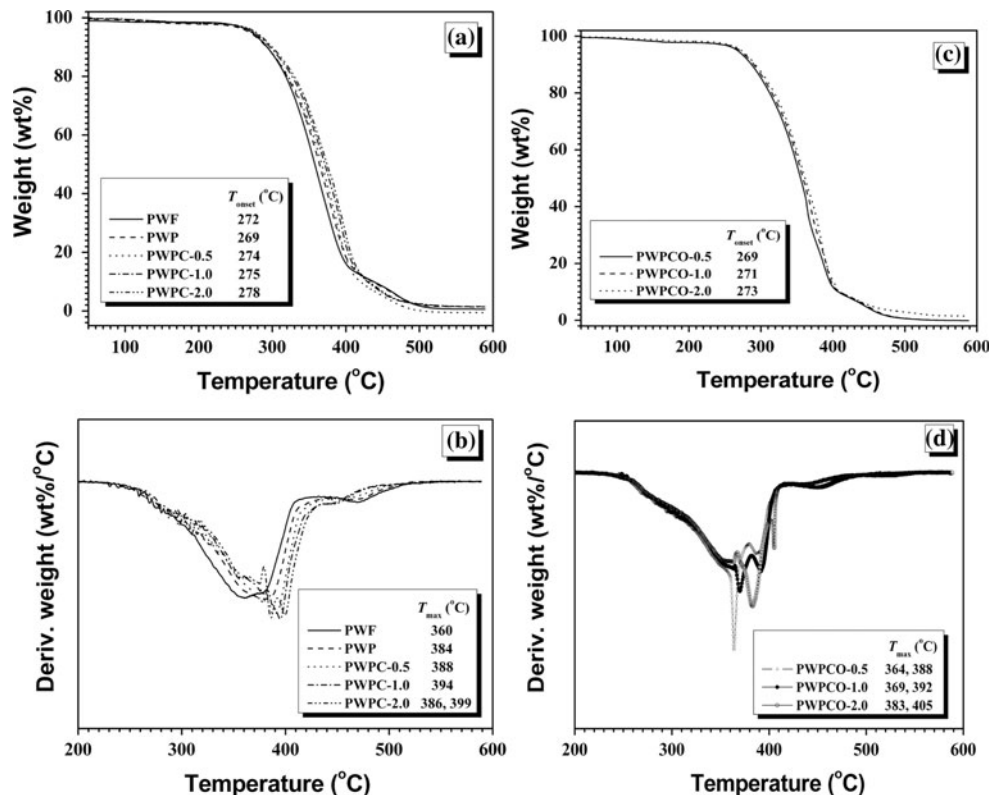
Incorporating pristine CNTs could further enhance the initial degradation temperature (T_{onset}) and T_{\max} of WPC, both of which were shifted to higher temperatures with the increase of CNTs loading level, for instance, at 1.0 wt% CNTs loading, T_{onset} and T_{\max} were increased by 5 °C and 10 °C relative to PWP (see Fig. 2a, b), which agreed well the reports in the literatures [18]. The improvements in

thermal stability were attributed to the barrier effects and radical-trapping effects of CNTs [18, 19]. Unexpectedly, CNT-OH led to a slightly earlier T_{onset} compared with CNTs at the same loading (see Fig. 2c), which was because that its thermal stability was poorer than pristine CNTs, which was reported previously by us [21]. In addition, two-step degradation of WPC took place in the presence of CNT-OH, which exhibited two T_{\max} s, for instance, 369 °C and 392 °C for 1.0 wt% CNT-OH filled WPC (Fig. 2d). At relatively lower loading, CNT-OH which resided in the interfaces almost did not contribute to the thermal stability of PP, and CNT-OH located in matrix was primarily responsible for conferring the thermal protection on PP. In contrast, CNTs exhibited better thermal protection for PP since they mainly resided in PP matrix. However, CNT-OH displayed a little better thermal barrier effects than pristine CNTs at relative higher loading. For instance, T_{\max} s of 2.0 wt% CNT-OH filled WPC were 383 °C and 405 °C, respectively, compared with 386 °C and 399 °C for WPC with 2.0 wt% CNTs.

Effects of CNTs or CNT-OH on flammability of WPC

The flammability properties of composites were evaluated by cone calorimeter testing [23, 24]. The evolution of heat release rate (HRR), especially its maximum peak (PHRR) was a very important parameter, and so was the time to

Fig. 2 TGA and DTG curves of all WPC samples



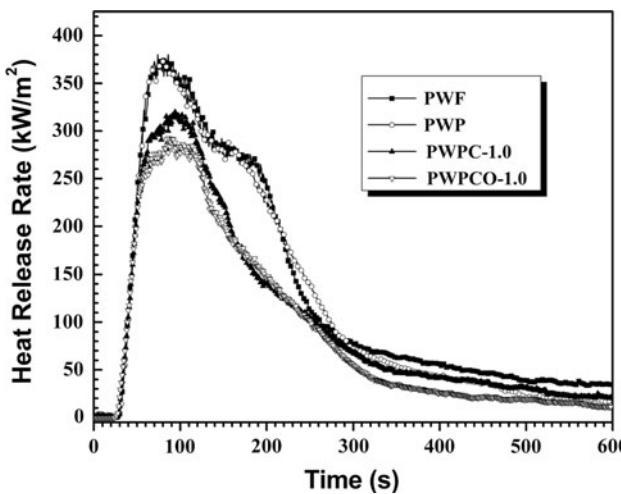


Fig. 3 Heat release rate curves for four typical WPC samples at a heat flux of 35 kW/m^2

ignition (t_{ign}), which represented the critical ignition temperature of a material. Figure 3 shows several typical heat release rate (HRR) curves for WPC, with detailed data summarized in Table 2. Compared with the noncompatibilized WPC, the WPC with PP-g-MA shared the similar PHRR value and other flammable parameters, which demonstrated that the compatibilizer did not influence the flammability of WPC. The addition of both pristine CNTs and CNT-OH resulted in slight shortening of the time to ignition, but reduced the PHRR and THR to different extents. Interestingly, each flammability parameter reached the respective optimum values for both WPC with 1.0 wt% CNTs and CNT-OH. For WPC, the presence of wood flour will affect the flammable behavior of PP/CNTs or CNT-OH, because they did not share similar thermal degradation and combustion mechanism. For example, 1.0 wt% CNTs could result in a 60% reduction in PHRR for PP [18, 19], while 1.0 wt% CNTs only reduced the PHRR value by 17% in the presence of 40 wt% wood flour. In the case of CNT-OH, it led to a 25% decrease in PHRR for WPC at

the same loading, which suggested that CNT-OH could confer better flame retardancy on WPC than did pristine CNTs due to its better dispersion in the matrix. Besides the reduction in PHRR, THR, and ASEA of WPC were also decreased to different degree with the incorporation of CNTs and CNT-OH, but CNT-OH caused a more reduction in both THR and ASEA values at the same loading.

Based on the above analysis, it was found that 1.0 wt% CNTs or CNT-OH loading was the optimum content for WPC. Since CNTs and CNT-OH could reduce the flammability of WPC, what was effect of its flame retardancy mechanism in the presence of high wood flour loading?

Flame retardancy mechanism and model

The currently accepted flame retardancy mechanisms of CNTs for polymer materials was the thermal barrier effect of CNTs network and radical-trapping effect. However, in WPC systems the presence of wood flour may influence the flame retardancy mechanism of CNTs, as a result, the mechanism may be somehow different and thus it is very necessary to understand the same.

In order to clarify the flame retardancy mechanism, it is usually useful to investigate the morphology and chemical structure of char residue after cone calorimeter measurements. Figure 4 shows the digital photos for char residues of different samples after cone calorimeter measurements. It was not difficult to observe that the morphologies of char for PWF and PWP were similar, and a small difference lied in that the char of PWP was more even than PWF, which demonstrated that the compatibilization reaction contributed to the homogeneity of char residue to some degree but did not conduce to the flame retardancy.

While for the char residue of PWPC-1.0 (WPC with 1.0 wt% CNTs) and PWPCO-1.0 (WPC with 1.0 wt% CNT-OH), more char were left and the char were much more compact relative to WPC without carbon nanotubes, which may be responsible for the improved flame

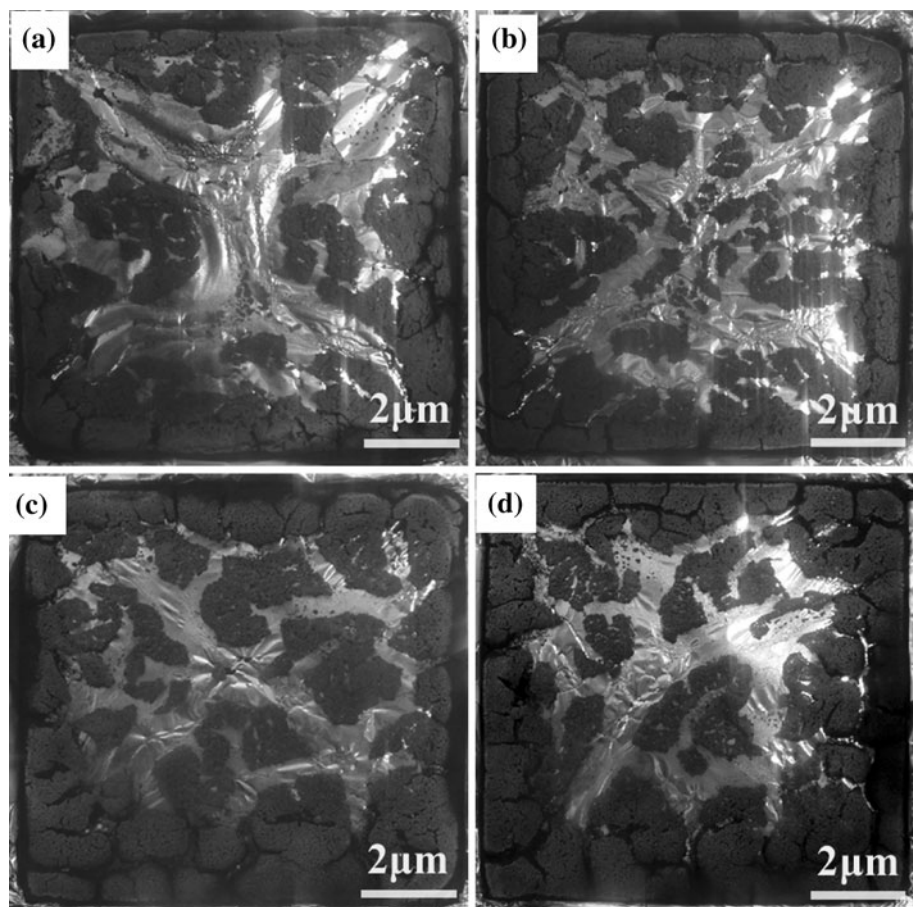
Table 2 Cone calorimeter data for WPC samples at a heat flux of 35 kW/m^2

Items	t_{ign} (s)	PHRR (kW/m^2)	AHRR (kW/m^2)	ASEA (m^2/kg)	THR (MJ/m^2)
PWF	26 ± 2	383 ± 15	135 ± 8	304 ± 10	77 ± 2
PWP	25 ± 2	375 ± 12	132 ± 7	306 ± 11	75 ± 2
PWPC-0.5	20 ± 1	320 ± 10	133 ± 8	319 ± 10	66 ± 2
PWPC-1.0	23 ± 2	318 ± 8	125 ± 7	280 ± 8	65 ± 1
PWPC-2.0	25 ± 2	327 ± 9	162 ± 9	340 ± 8	66 ± 2
PWPCO-0.5	23 ± 2	292 ± 7	180 ± 11	314 ± 7	60 ± 1
PWPCO-1.0	23 ± 2	285 ± 7	143 ± 8	254 ± 6	56 ± 1
PWPCO-2.0	25 ± 2	287 ± 6	148 ± 9	316 ± 8	58 ± 1

Note: All data reported here were the average values

t_{ign} time to ignition, PHRR peak heat release rate, AHRR average heat release rate, ASEA average specific extinction area, THR total heat release

Fig. 4 Digital photos for four typical WPC samples after cone calorimeter measurements at a heat flux of 35 kW/m^2



retardancy. However, no obvious difference in the char residues was observed between PWPC-1.0 and PWPCO-1.0, which was also consistent to those of PWF and PWP.

Digital photos only provide the visual observation, not the micromorphologic observation on char, and cannot distinguish the slight differences between different char residues. In this context, SEM observation offers another more powerful tool to determine the micromorphology of char surface. From the Fig. 5 which shows the surface micromorphology of char residue for PWF and PWP, it is apparent that the char of PWP displays a more compact surface compared to that of PWF both at low and higher magnifications, which may help us understand the slight improvement in thermal oxidation stability and flame retardancy of WPC.

For the chars of PWPC-1.0 and PWPCO-1.0, some tiny cracks could be observed on the char residue for PWPC-1.0 at low magnification (see Fig. 6a). By contrast, intact and compact chars are seen for PWPCO-1.0 (see Fig. 6c). At higher magnification, we could observe that CNTs seemed to grow up from the char (see Fig. 6b), while CNT-OH did not (see Fig. 6d), which was because of the fact that compared with pristine CNTs, better interfacial adhesion of CNT-OH with wood flour could result in more

homogenous dispersion in char residue after cone measurements, and consequently CNT-OH was embedded in the char while CNTs grew up from the char. The former structure could not effectively reinforce the char layer, while the CNT-OH penetrated in the char in the latter one and consequently could effectively seal and consolidate the char. Thus, CNT-OH could confer better flame retardancy on WPC than did CNTs.

It was not enough only investigate the morphology of char for clarifying the flame retardancy mechanism of CNTs or CNT-OH in the presence of wood flour. IR spectra of char also could provide the information on the chemical structure of char residues. As shown in Fig. 7, the IR spectra of char for PWF and PWP are somewhat similar; the characteristic absorption peaks of benzene ring and substituted benzene derivatives are observed at $1400\text{--}1610 \text{ cm}^{-1}$, 1260 cm^{-1} , and 795 cm^{-1} . The C–O stretching vibration mode at $1010\text{--}1140 \text{ cm}^{-1}$ is also observed. In addition, the typical vibration peak of Si–O appeared at around 465 cm^{-1} [3, 25]. The characteristic absorption peaks at 1260 cm^{-1} and 795 cm^{-1} do not appear in the IR spectrum of PWP, which indicates that the char may not contain substituted benzene derivatives. Whatever, these analyses implied that the char primarily consisted of

Fig. 5 SEM images of char residues for **a, b** PWF and **c, d** PWP

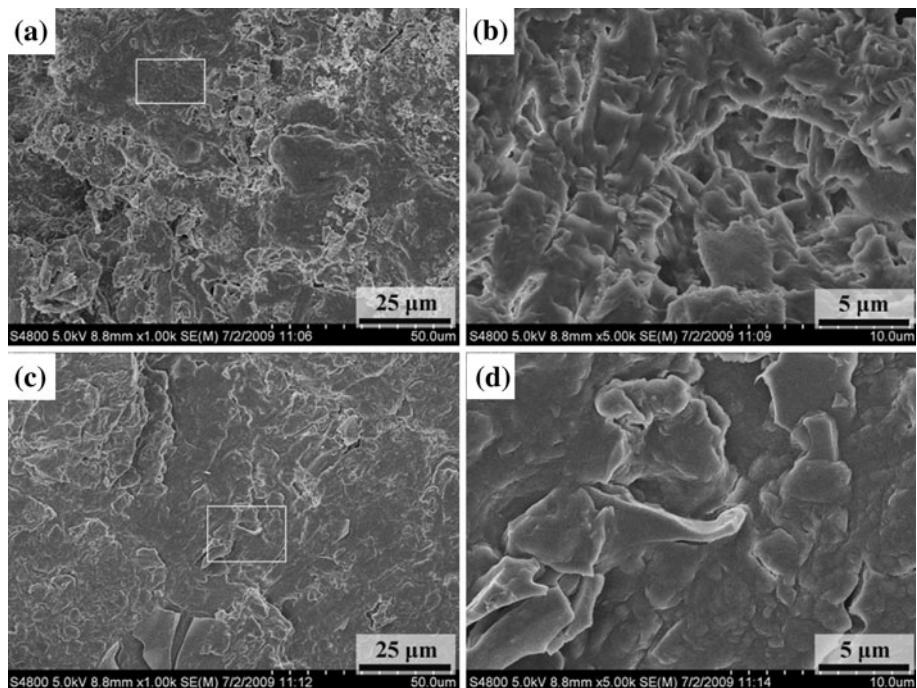
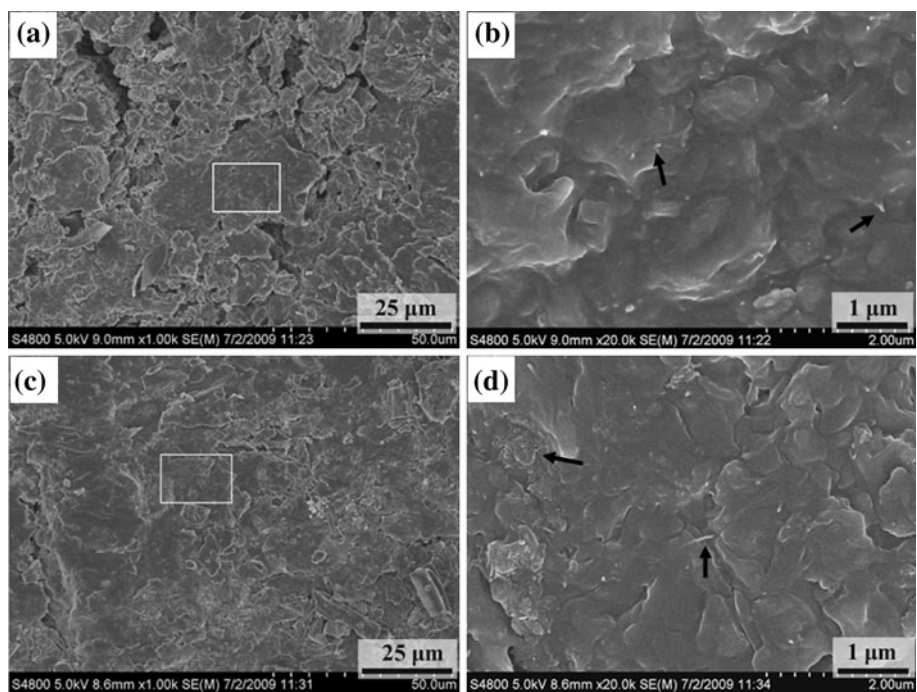


Fig. 6 SEM images of char residues for **a, b** PWPC-1.0 and **c, d** PWPCO-1.0



benzene derivatives, SiO_2 and small amounts of other substances.

For the IR spectra of char for WPC with CNTs and CNT-OH, PWPC shared rather similar IR absorption features indicating their similar chemical structure. One difference was the appearance of the absorption peak of carbonyl groups on CNTs walls near 1650 cm^{-1} [26] for

PWPC, demonstrating that its char was composed of CNTs components, and the result was consistent with above SEM observations. Interestingly, besides some peaks observed as above, some new peaks appeared in the IR spectrum of the char for WPC with CNT-OH. Broad absorption band at $3300\text{--}3600 \text{ cm}^{-1}$ and 1418 cm^{-1} indicated the existence of $-\text{OH}$, the characteristic stretching vibration peak of

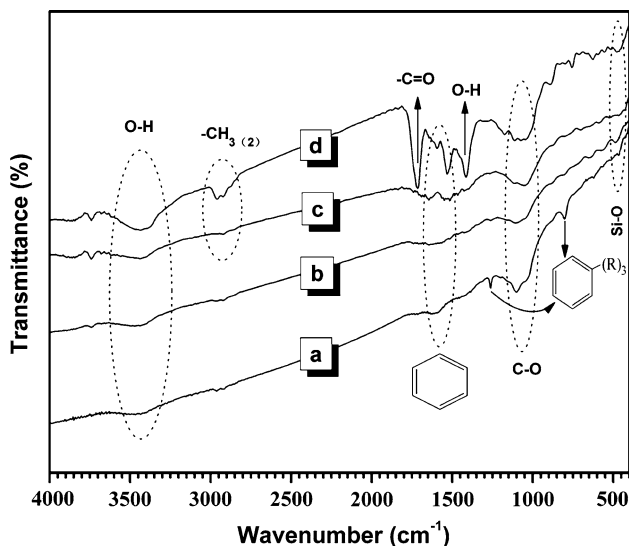


Fig. 7 IR spectra of char residue for (a) PWF, (b) PWP, (c) PWPC-1.0, and (d) PWPCO-1.0

carbonyl groups ($\text{C}=\text{O}$) at 1720 cm^{-1} was clearly observed. Furthermore, absorption peaks at 2920 cm^{-1} and 2961 cm^{-1} attributed to the methyl or methylene groups ($-\text{CH}_3$ or $-\text{CH}_2-$) also appeared. These observations implied that the char of PWPCO contained alkyl groups, carbonyl groups, hydroxyl groups, and other chemical groups, as well as SiO_2 . On the other hand, it also suggested of the better thermal insulation effect due to CNT-OH than due to CNTs, and it was not difficult to understand the better flame retardancy mechanism on WPC conferred by CNT-OH.

On the basis of the above surface morphology and chemical structure analysis, we proposed a combustion

model for four typical WPC samples, as shown in Fig. 8. The model will help us to understand the flame retardancy mechanism of CNTs and CNT-OH for WPC. In the model (see Fig. 8a, b), though the addition of compatibilizer improved the dispersion of wood flour in the polymeric matrix, and even the dispersion of char residue of WPC during cone calorimeter measurements, it still did not contribute to the flame retardancy since PP-g-MA could not provide the thermal protection for WPC in a fire. While for WPC with CNTs and CNT-OH (see Fig. 8c, d), during cone calorimeter measurements, CNTs or CNT-OH networks could effectively act as thermal barrier for the underlying WPC materials; on the other hand, they could also terminate the active radicals created in the process of thermal degradation of PP matrix, both of which contributed to the flame retardancy of WPC. As for the difference between CNTs and CNT-OH, the better interfacial compatibilization of CNT-OH in the WPC resulted in better thermal barrier effects and further more compact and intact char residue layer, which explained why better flame retardancy offered by CNT-OH is more superior than pristine CNTs.

Conclusions

In this study, we investigated the effects of pristine CNTs and hydroxylated CNTs (CNT-OH) on the thermal oxidative stability and flame retardancy of WPC materials. The presence of both CNTs and CNT-OH could enhance the thermal stability of WPC, especially the maximum weight loss rate temperature, and the enhancement in thermal properties of WPC was slightly better at relative high loading level. Incorporating CNTs and CNT-OH could effectively reduce the flammability of WPC, and CNT-OH conferred better flame retardancy on WPC relative to pristine CNTs due to its improved interfacial compatibilization between CNT-OH and wood flour as well as the polymer matrix.

Acknowledgements This study was supported by the Key Program of Science & Technology Bureau of Zhejiang Province, China (Grant No. 2007C12018).

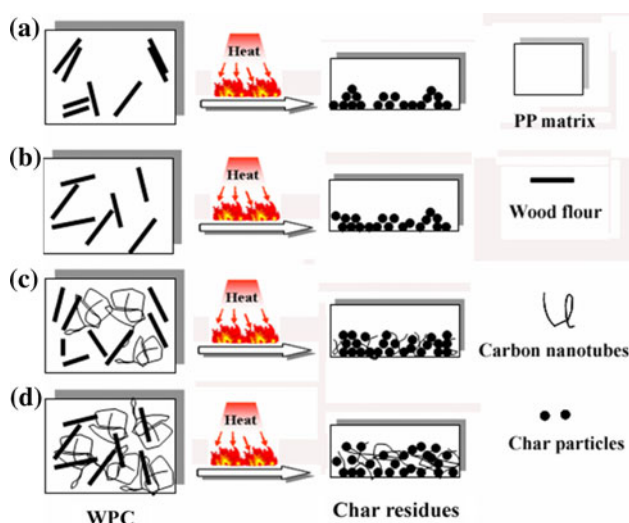


Fig. 8 Schematic representation for the flame retardancy models of four kinds of WPC, (A) PWF, (B) PWP, (C) PWPC-1.0, and (D) PWPCO-1.0

References

- Balatinecz JJ, Woodhams RT (1993) J Forestry 91:22
- Zhao YS, Wang KJ, Zhu FH, Xue P, Jia MY (2006) Polym Degrad Stab 91:2874
- Liao HT, Wu CS (2005) Macromol Mater Eng 290:695
- Guo G, Park CB, Lee YH, Kim YS, Sain M (2007) Polym Eng Sci 47:330
- Dominkovics Z, Dózsa L, Pukánszky B (2007) Compos A 38:1893

6. Balasuriya P, Ye L, Mai Y, Wu J (2002) *J Appl Polym Sci* 83:2505
7. Razi PS, Raman A (2000) *J Compos Mater* 34:980
8. Liao B, Huang Y, Cong G (1997) *J Appl Polym Sci* 66:1561
9. Rodríguez CA, Medina JA, Reinecke H (2003) *J Appl Polym Sci* 90:3466
10. Beyer G (2002) *Plast Addit Compound* 4:22
11. Anna P, Zimonyi E, Marton A, Szep A, Matko S, Keszei S, Bertalan G, Marosi G (2003) *Macromol Symp* 202:245
12. Oladipo AB, Wichman IS (1999) *Combust Flame* 118:317
13. Pandey JK, Reddy KR, Kumar AP, Singh RP (2005) *Polym Degrad Stab* 88:234
14. Giannelis EP (1996) *Adv Mater* 8:29
15. Zhu J, Wilkie CA (2000) *Polym Intern* 49:1158
16. Morgan AB (2006) *Polym Adv Technol* 17:206
17. Kashiwagi T, Gruke E, Hilding J, Groth K, Harris R, Butler K, Shields J, Kharchenko S, Douglas J (2004) *Polym Degrad Stab* 45:4227
18. Kashiwagi T, Gruke E, Hilding J, Groth K, Harris R, Awad W, Douglas J (2002) *Macromol Rapid Commun* 23:761
19. Kashiwagi T, Du F, Winey KI, Groth KM, Shields J, Bellayer SP, Kim H, Douglas JF (2005) *Polymer* 45:471
20. Guo G, Wang KH, Park CB, Kim YS, Li G (2007) *J Appl Polym Sci* 104:1058
21. Song PA, Xu LH, Guo ZH, Zhang Y, Fang ZP (2008) *J Mater Chem* 18:5083
22. Hristov V, Vasileva S (2003) *Macromol Mater Eng* 288:798
23. Zhu J, Morgan AB, Lamelas FJ, Wilkie CA (2001) *Chem Mater* 13:3774
24. Zenetti M, Kashiwagi T, Falqui L, Camino G (2002) *Chem Mater* 14:881
25. Lee DC, Jang LW (1996) *J Appl Polym Sci* 61:1117
26. Colthup NB, Daly LH, Wiberley SE (1975) *Introduction to infrared and Raman spectroscopy*. Academic press, New York